Journal of Drug Delivery Science and Technology 113 (2025) 107342

Contents lists available at ScienceDirect

Journal of Drug Delivery Science and Technology

journal homepage: www.elsevier.com/locate/jddst

Multicomponent nasal spray delivered via penetration-enhancer containing vesicles (PEVs) for antioxidant and antibacterial protection

Rita Abi Rached [a,b], Ashok K. Shakya [c,d], Maria Letizia Manca [a,*], Matteo Aroffu [a], Fátima García-Villén [e], Joe A. Touma [f], Xavier Fernàndez-Busquets [g,h], Marija Ivanov [i], Jose Luis Pedraz [j], Nicolas Louka [b], Richard G. Maroun [b], Maria Manconi [a]

[a] Department of Life and Environmental Sciences, University of Cagliari, University Campus, S.P. Monserrato-Sestu Km 0.700, 09042, Monserrato, CA, Italy
[b] Centre d'Analyses et de Recherche, Unité de Recherche TVA, Laboratoire CTA, Faculté des Sciences, Université Saint-Joseph de Beyrouth, B.P. 17-5208 Riad El Solh, Beirut, 1104 2020, Lebanon
[c] Pharmacological & Diagnostic Research Center, Faculty of Pharmacy, Al-Ahliyya Amman University, Amman, 19328, Jordan
[d] Michael Sayegh Faculty of Pharmacy, Aqaba University of Technology, South Beach Road, Aqaba, 11191, Jordan
[e] Department of Pharmacy and Pharmaceutical Technology, School of Pharmacy, University of Granada, Campus of Cartuja, 18071, Granada, Spain
[f] Château Saint Thomas, Bekaa Valley, Kab Elias, Lebanon
[g] Institute for Bioengineering of Catalonia (IBEC), The Barcelona Institute of Science and Technology, Baldiri Reixac 10-12, 08028, Barcelona, Spain
[h] Barcelona Institute for Global Health (ISGlobal), Hospital Clínic-Universitat de Barcelona, Rosselló 149-153, 08036, Barcelona, Spain
[i] Institute for Biological Research "Siniša Stanković", National Institute of the Republic of Serbia, University of Belgrade, Bulevar despota Stefana 142, Belgrade, 11108, Serbia
[j] NanoBioCel Group, Laboratory of Pharmaceutics, School of Pharmacy, University of the Basque Country (UPV/EHU), Biomedical Research Center in Bioengineering, Biomaterials and Nanomedicine (CIBER-BBN), BioAraba, NanoBioCel research Group, Vitoria-Gasteiz, Spain

ARTICLE INFO

Keywords:
Grape seeds
Phospholipid vesicles
PG-PEVs and carrageenan-PG-PEVs
Nasal spray
Droplet distribution
Oxidative stress
Staphylococcus aureus

ABSTRACT

In this study, a nasal spray was formulated and tested co-loading grape seed extract, thymol, and camphor in penetration enhancer containing vesicles (PEVs) tailored to synergistically protect the nasal mucosa against oxidative stress and bacterial colonization. Based on their previously demonstrated effects, PEVs were prepared with propylene glycol (PG) and further enriched with carrageenan to promote muco-adhesion. The mean diameter of PG-PEVs was ~177 nm, and that of carrageenan PG-PEVs was ~194 nm. The polydispersity index ranged from 0.25 to 0.27, confirming the homogeneity of the dispersions. The zeta potential was significantly negative (~−63 mV) and the entrapment efficiency was ~88 %, irrespective of vesicle composition. Sprayability studies disclosed that both PG-PEVs and carrageenan-PG-PEVs generated droplets larger than 10 μm, thus appropriate for the deposition in the nasal cavity. Regional nasal deposition studies, carried out with a realistic nasal replica, highlighted that formulation droplets were deposited in the vestibule and turbinate areas of the nose. The ability of formulations to inhibit protein denaturation confirmed their anti-inflammatory effects. *In vitro* study with A549 and CuFi-1 cells, underlined that PG-PEVs and especially carrageenan PG-PEVs were non-toxic (viability ~ 140 %) and effectively counteracted cell apoptosis caused by hydrogen peroxide, restoring healthy conditions. The *in vivo* study in mice demonstrated that grape seed extract, thymol, and camphor-loaded carrageenan PG-PEVs were highly effective in counteracting the proliferation of *Staphylococcus aureus*.

* Corresponding author.
E-mail addresses: rita.abirached@unica.it (R. Abi Rached), ak_shakya@ammanu.edu.jo (A.K. Shakya), mlmanca@unica.it (M.L. Manca), matteo.aroffu@unica.it (M. Aroffu), fgarvillen@ugr.es (F. García-Villén), joe@clossthomas.com (J.A. Touma), xfernandez@ibecbarcelona.eu (X. Fernàndez-Busquets), marija.smiljkovic@ibiss.bg.ac.rs (M. Ivanov), joseluis.pedraz@ehu.eus (J.L. Pedraz), nicolas.louka@usj.edu.lb (N. Louka), richard.maroun@usj.edu.lb (R.G. Maroun), manconi@unica.it (M. Manconi).

https://doi.org/10.1016/j.jddst.2025.107342
Received 16 April 2025; Received in revised form 28 July 2025; Accepted 30 July 2025
Available online 31 July 2025

1. Introduction

1.1. The nasal cavity as a barrier and target for therapy

The nasal cavity is the most cephalic part of the respiratory tract, communicating with the external environment and is a critical site for the conditioning of inhaled air through its humidification, warming, and filtration [1]. This functional filtration removes harmful chemicals or microbes, thereby protecting the more sensitive tissues in the lower tracheobronchial and pulmonary airways. However, it can also be a prime target for many inhaled toxicants that may cause acute, subacute, or chronic rhinitis in the nasal cavity, sinusitis in the paranasal sinuses, and rhinosinusitis in both sites [2]. The latter is a heterogeneous group of disorders affecting approximately 5–15 % of the global population with a significant impact on the quality of life [3]. Traditionally attributed to viral, fungal, or bacterial infection, it is now widely accepted that these conditions are closely linked to immunological and inflammatory factors [4]. Common current treatments and alternative approaches for rhinitis and rhinosinusitis include systemic medications such as antibiotics, anti-histaminics, and steroids, which eliminate infection, reduce inflammation, and restore the physiological state of nasal mucosa.

As an alternative, nasal sprays in solutions or in vesicle-based formulations have gained prominence for localized delivery of drugs and natural compounds, providing relief from acute or chronic congestions or obstructions [5]. In recent years, natural formulations have been reevaluated for their therapeutic properties, but especially because of the growing market demand and advances in pharmacological and medical research [6].

Various strategies have been developed for both regeneration of injured tissues and improvement of antibacterial effectiveness by using either natural or synthetic biomaterials that may be also tested for nasal application [7–12].

Among the different formulations for nasal delivery of natural compounds, vesicular systems have shown promise for the treatment of rhinitis due to their moisturizing and hydrating properties. Composed of phospholipids naturally present in nasal mucosa, making up approximately 75 % of its protective nasal surfactant layer [13], vesicles can support mucociliary clearance and maintain nasal functions. More recently, these benefits have been enhanced with the introduction of hyalurosomes, special phospholipid vesicles immobilized with sodium hyaluronate, which further support the nasal barrier [14]. Liposomes and hyalurosomes have been tested in nasal sprays with the double objective of improving mucosal health and delivering natural chemicals. In a previous study, hyalurosomes were used to deliver an extract of *Zingiber officinale* with anti-inflammatory and antioxidant properties [15], yielding formulations that remained stable upon storage and effectively deposited in the anterior part of the nasal cavity. Similarly, sprayable, biocompatible and effective nasal spray formulations for the treatment of nasopharyngeal diseases were obtained by using penetration enhancer-containing vesicles (PEVs) to deliver the active molecules contained in the extract of *Cardiospermum halicacabum* L. (*C. halicacabum*) [16].

PEVs, along with various phospholipid-based means of delivery, have attracted interest as ultra-deformable vesicles containing chemical penetration enhancers directly into the lipid bilayer. This innovative dual-function system merges the structural flexibility of deformable vesicles with the biological activity of the enhancers, creating a synergistic effect that significantly enhances their ability to cross the biological barrier [17–21]. The penetration enhancers used in PEVs, such as surfactants, terpenes, ethanol, or glycol, not only increase vesicle deformability, but also temporarily disrupt the structure of biological membranes, facilitating the passage of both the carrier and the encapsulated drug [19,22].

1.2. Sustainability: grape pomace as a source of natural chemicals

Despite the potential benefits, research on the efficacy of nasal sprays formulated with liposomes, hyalurosomes, PEVs, or other phospholipid vesicles containing natural molecules or extracts remains still limited. This gap is significant as such formulations could represent valuable candidates for local nasal therapy. In this context, extracts derived from agri-food side-streams, have emerged as a sustainable and cost-effective source of natural chemicals, aligning with the principles of the circular economy and the European Agenda 2030. Among these, grape pomace is one of the most extensively studied due to its richness in antioxidants (1–2 % of phenolic compounds) and its widespread availability [23–26]. Composed of skin, stalks, seeds, grape pomace also contains 30 % of neutral polysaccharides, 20 % of pectic substances, 15 % structural proteins and fibers, and unsaturated fatty acids such as linoleic acid (58–78 %) and oleic acid (15–20 %), and saturated lipids such as palmitic acid (7–10 %) and stearic acid (4–6 %) [27].

1.3. Aim of the study

Building upon this promising perspective, the present study aimed to obtain antioxidant and anti-inflammatory extract from the seeds of *Obeidi* grape pomace and co-load it with thymol and camphor. The formulations were further optimized using propylene glycol (PG) to obtain Penetration enhancer containing vesicles, so-called PG-PEVs, aiming at improving diffusion-enhancing properties across the nasal membrane [28]. PEVs were further enriched with carrageenan, as a mucoadhesive and stabilizer agent, to obtain carrageenan PG-PEVs [29,30]. The physico-chemical (size, zeta potential, polydispersity index) and technological characteristics (entrapment efficiency, sprayability, and regional deposition) of the obtained formulations were measured. Their potential anti-inflammatory effects were assessed via the protein denaturation inhibition assay, while their biocompatibility was tested on human lung adenocarcinoma epithelial cells (A549) and cystic fibrosis cells (CuFi-1) along with their protective effect against oxidative stress induced by hydrogen peroxide. The antibacterial effects were tested both *in vitro* and *in vivo*, providing a comprehensive evaluation of the potential of these sustainable formulations for nasal therapy.

2. Materials & methods

2.1. Materials

Lipoid S75, a mixture of soybean-derived phospholipids, triglycerides, and fatty acids, was purchased from Lipoid (Ludwigshafen, Germany). Ethanol, propylene glycol, and all other analytical grade reagents were obtained from Sigma-Aldrich (Milan, Italy), while thymol (≥99.5 % purity) and camphor (96 % purity) were sourced from Sigma-Aldrich (St. Louis, MO, USA). Ultrapure water was produced using a Milli-Q system (Milford, MA, USA).

2.2. Plant material

Pomace from the autochthonous Obeidi grape variety was provided by Château Saint-Thomas, a vineyard located in Lebanon's Beqaa Valley (Latitude: 34.008889; Longitude: 36.145278). This rare variety, considered purely Lebanese due to its unique DNA profile, was collected post-winemaking as a 'first waste' material. Pomaces were dried in an airflow oven at 50 °C for 48 h. Seeds were then manually separated from the skins, ground, and sieved to obtain particles between 850 and 425 μm [31]. The processed seeds were placed in plastic bags at ambient temperature in obscurity. Though primarily used in winemaking, Obeidi seeds retain valuable constituents, such as fatty acids (13–19 %), proteins (11 %), carbohydrates (60–70 %), and polyphenols (5–8 %), making them a rich by-product for further valorization [32,33].

2.3. Cell culture reagents

A549 (ATCC® CCL-185™) and CuFi-1 (ATCC® CRL-4013™) cell lines were obtained from the American Type Culture Collection (ATCC; Manassas, VA, USA). Culture reagents including Kaighn's modification of Ham's F-12 medium with L-glutamine, penicillin-streptomycin, fetal bovine serum (FBS), Dulbecco's phosphate-buffered saline (DPBS), and trypsin-EDTA (0.5 %) without phenol red were purchased from Gibco™ (Life Technologies, Madrid, Spain). Serum-free Bronchial Epithelial Growth Medium (BEGM BulletKit; CC-3170) and SingleQuot supplements were sourced from Lonza (Clonetics, Lonza Walkersville Inc.; Walkersville, MD, USA). Dimethyl sulfoxide (DMSO) was obtained from Scharlau (Madrid, Spain). Human placental collagen type IV (Sigma, Cat. No. C-7521) and the Cell Counting Kit-8 (CCK-8) were purchased from Sigma-Aldrich (St. Louis, MO, USA).

2.4. Extraction procedure

The Obeidi extract was prepared as reported in a previous work [34]. Briefly, 1 g of ground grape seeds was dispersed in 10 mL of an ethanol: water solution (8:2, v/v). The mixture was incubated for 2 h at 50 °C in a digital water bath (JSWB-22T, JS Research Inc., Gongju-City, Korea). Ethanol was then removed by rotary evaporation at 50 °C under reduced pressure. The remaining aqueous phase was spray-dried using an automated atomizer (Shanghai Attainpak, China), yielding a fine powder extract composed of small and uniform particles.

2.5. Characterization of extract

2.5.1. Determination of total phenolic compounds

The total polyphenol content was quantified using the Folin–Ciocalteu colorimetric assay [35], with gallic acid as the standard. Briefly, 200 µL of the extract solution (0.1 g/mL) was mixed with 1 mL of Folin–Ciocalteu reagent (Sigma-Aldrich, Darmstadt, Germany) and 800 µL of sodium carbonate solution (Sigma-Aldrich, Darmstadt, Germany). The mixture was heated at 60 °C for 10 min, then cooled for an additional 10 min. Absorbance was measured at 750 nm using a spectrophotometer (Shimadzu UV-1800 spectrophotometer, Japan).

2.5.2. Determination of antioxidant activity

2.5.2.1. Diphenyl-2-picrylhydrazyl (DPPH) free radical scavenging activity. The antioxidant activity of the grape seed extract was first evaluated using the DPPH (2,2-diphenyl-1-picrylhydrazyl) radical scavenging method. A volume of 1450 µL of DPPH solution (0.06 mM) was added to 50 µL of either the extract in dispersion or a Trolox standard [36]. After incubation in the dark at room temperature for 30 min, the absorbance was estimated at a wavelength of 515 nm. A calibration curve was generated using various concentrations of Trolox. The percentage of radical inhibition, expressed as antioxidant activity, was calculated using the following equation:

$$\textbf{Antioxidant activity}\ (\%) = \frac{(\textbf{absorbance of DPPH solution} - \textbf{absorbance of sample})}{\textbf{absorbance of DPPH solution}} \times 100$$

2.5.2.2. Cupric ion reducing antioxidant capacity assay (CUPRAC). CUPRAC analysis was performed using a commercial kit (Bioquochem, Asturias, Spain), based on the reduction of a copper(II)-neocuproine complex. Briefly, 40 µL of extract in dispersion (0.1 g/mL) or Trolox standard were mixed with 200 µL of the reagent solution. After 30 min of incubation at room temperature, absorbance was recorded at 450 nm using a microplate reader (Synergy 4, Synergy ™ Multi-Detection Microplate Reader, Bio-Tek Instruments, AHSI SPA, Bernareggio, Italy). Results were expressed as mM of Trolox equivalents [37].

2.5.2.3. Ferric reducing antioxidant power assay (FRAP). The FRAP assay was carried out using the Bioquochem kit (Asturias, Spain) to evaluate the ability of the extract to reduce ferric (Fe^{3+}) to ferrous (Fe^{2+}) ions under acidic conditions. A volume of 10 µL of the extract solution (0.1 g/mL) or Trolox standard was added to 220 µL of the FRAP reagent mixture. The absorbance was measured at 593 nm after 4 min of stirring. The antioxidant activity was reported as µM of Fe^{2+} equivalents [38].

2.5.3. Acquisition of infra-red spectra

The infra-red spectra of dried samples were recorded using a PerkinElmer Spectrum II-FT-IR Spectrometer (USA) between 4000 cm^{-1} to 500 cm^{-1}. Anhydrous KBr tablets with spectroscopic grade were used to prepare the dried extract for analysis.

2.5.4. Analysis of extract with Gas Chromatography-Mass Spectroscopy (GC-MS)

A Shimadzu QP2020 GC-MS (Kyoto, Japan) coupled with a split-split-less injector and DB5 MS fused silica column (5 % phenyl, 95 % polydimethylsiloxane coated 30 m × 0.25 mm capillary column, film thickness 0.25 µm) was used. To separate the components, a linear temperature program was applied at a heating rate of 7 °C/min, starting from 50 °C up to 280 °C, and maintaining the system at 280 °C for a total runtime of 74 min. The injector temperature was 260 °C with a split ratio of 20:1; the injection volume was 1 µL of a 2 mg sample treated with 100 µL of derivatizing reagent at 60 °C, and helium was the carrier gas. The source and detector temperature of mass spectroscopy was 240 °C; the interface temperature was 250 °C; the ionization energy was 70 eV; the atomic mass unit gain was −492 and offs were −67; the scan range was 35–500 atomic mass units (amu), with a scan speed of 1666. The solvent cut was 3 min, and the data were collected from 4.5 min. The mass spectrum of each molecule was compared to the matching documented spectra in NIST and ADAMS libraries [39]. The relative retention indices of molecules were additionally validated through the comparison with published data of n-alkanes (C8-C35) from the Adam library [40]. The compounds were identified by comparing their retention times (Rt) with those of standard molecules, assessing their linear indices relative to a series of n-hydrocarbons.

2.5.5. Analysis of extract with Liquid Chromatography-Mass Spectroscopy (LC-MS)

Phenolic compounds in the extract were separated and identified using ultra-performance liquid chromatography (UPLC: a SciEx system, Exion-UPLC, USA), equipped with Analyst 1.7 software and an LC-ESI-MS/MS-4500-QTRAP system (AB SciEx Instruments, Framingham, MA, USA). Chromatographic separation was performed at 50 °C using an ODS column (100 × 2.1 mm, 5 µm). The mobile phase A consisted of water with 1 % formic acid and mobile phase B of methanol with 1 % formic acid. A gradient program was applied as follows: 80 % A and 20 % B at 0 min; 80 % A and 20 % B at 1 min; 0 % A and 100 % B at 12 min; 0 % A and 100 % B at 18 min; 80 % A and 20 % B at 19 min; and 80 % A and 20 % B at 22 min. The solvent flow rate was set at 0.35 mL/min with a 5 µL injection volume with sample concentration of 1 mg/mL.

Calibration curves were built using increasing concentrations of each phenolic standard (0.25–0.015 mg/mL). For each curve, an equation was obtained and the R2 was calculated [41].

2.6. Preparation and characterization of vesicles

2.6.1. Preparation

To prepare PG-PEVs, *Obeidi* extract (10 mg/mL), phospholipid S75 (90 mg/mL), thymol (10 mg/mL), and camphor (10 mg/mL) were weighed in a glass vial and hydrated with an aqueous solution of propylene glycol (30 % v/v). To prepare carrageenan PG-PEVs, 2 mg/mL of carrageenan was dispersed in the aqueous solution of propylene glycol (30 % v/v) and used as a hydrating medium for the different components. Both PG-PEVs and carrageenan PG-PEVS were sonicated (30 cycles, 5 on and 2 off, probe amplitude 13 μm) with a Soniprep 150 sonicator (MSE; Crowley, London, UK) and were stored at 4 °C after preparation.

2.6.2. Evaluation of physico-chemical properties

The vesicle morphology was observed by cryogenic transmission electron microscopy (cryo-TEM) in a Tecnai G2 20 Twin equipment (FEI Company; Hillsboro, OR, USA), at a voltage of 200 KeV. 3 μL of the sample was placed on glow-discharged 300 mesh Quantifoil TEM grid, and excess liquid was eliminated with filter paper. The grid was plunge-frozen into liquid ethane in a FEI Vitrobot Mark IV (Eindhoven, The Netherlands), transported to a 626 DH Single Tilt Cryo-Holder (Gatan, France), kept beneath −170 °C and finally transferred to the microscope at liquid nitrogen temperature (−196 °C).

The mean diameter and polydispersity index of vesicles were measured with a Zetasizer Ultra (Malvern Instruments; Worcestershire, UK) based on their ability to scattering the light. The zeta potential of vesicles was measured with the same apparatus as a function of their electrophoretic mobility. Vesicular dispersions were diluted 1:100 in water before measurements to be optically clear, avoid the attenuation of the laser beam by the particles and prevent the reduction of the scattered light that can be detected [42].

The vesicles were purified from the non-incorporated molecules by dialysis (Spectra/Por® membranes, 3 nm pore size, 12–14 kDa, Spectrum Laboratories Inc.; Rancho Dominguez, CA, USA). Samples (1 mL) were placed inside the membrane and immersed in 1 L of water at room temperature for 2 h. The water was refreshed every hour to ensure the complete removal of unentrapped molecules [43]. The antioxidant activity was evaluated before and after dialysis as reported in section 2.5.2.

2.6.3. Evaluation of stability

Vesicles were stored at 4 °C for 12 months, and their size and polydispersity index were measured at scheduled time points using the Zetasizer Ultra, as described in Section 2.6.2.

2.6.4. Measurement of sprayability

The size distribution of droplets generated by spraying the vesicle dispersions was assessed by laser diffraction, using the Spraytec® (Malvern Panalytical Ltd., Malvern, United Kingdom), which detects droplets sized from 0.1 to 2000 μm. Tests were carried out in triplicate, placing the samples at 4 and 7 cm starting from the nozzle output and rotating 45° the spray device, according to established protocols [16,39]. The equipment provided D10, D50, and D90 values, corresponding to 10 %, 50 %, and 90 % of the overall volume of undersized particles. To quantify the distribution, span, defined as (D90−D10)/D50, was further calculated.

2.6.5. Regional deposition of droplets

The regional deposition of vesicles was assessed with the realistic nasal replica Alberta Idealized Nasal Inlet, quantifying the amount of extract recovered in each region (vestibule, olfactory region, turbinate, and nasopharynx) after spraying. The Alberta Idealized Nasal Inlet was connected to the Next Generation Impactor (Copley, Eur. Ph 7.2, Copley Scientific Ltd., Nottingham, UK) [44,45], and to a vacuum pump operating at a 7.5 mL/min flow rate, which mimics a steady and slow inhalation through a nostril [46]. Samples were transferred into a commercial device (Nasonex®) and 5 actuations were made positioning the device at 45° or 60° to the nasal replica. A glass collector was held below the inlet to collect any formulation that may have dripped out of the vestibule. After the deposition of the droplets, each region was washed with an appropriate volume of methanol allowing the disruption of the vesicles and the recovery of the extract. The amount of extract deposited was determined at the maximum adsorption wavelength (290 nm) using a microplate reader (Synergy 4, Synergy ™ Multi-Detection Microplate Reader, Bio-Tek Instruments, AHSI SPA, Bernareggio, Italy).

2.7. Inhibition of protein denaturation of extract in dispersion or loaded in vesicles

0.45 mL of bovine serum albumin (BSA) (5 % w/v aqueous solution) and 0.05 mL of vesicles (250 μg/mL) compose the test solution (0.5 mL); 0.45 mL of BSA (5 % w/v aqueous solution) and 0.05 mL of distilled water constitute the test control solution (0.5 mL); 0.45 mL of distilled water and 0.05 mL of vesicles (250 μg/mL) serve as the product control solution (0.5 mL); 0.45 mL of BSA (5 %w/v aqueous solution) and 0.05 mL of diclofenac sodium (250 μg/mL) form the standard solution (0.5 mL). Using 1 N hydrochloric acid, the pH of each of the dispersions was adjusted to 6.3. After 20 min of incubation at 37 °C, the temperature was raised to maintain the samples at 57 °C for 3 min. The mentioned solutions were mixed with 2.5 mL of phosphate buffer saline (pH ~7.4, ~150 mM of total salts) after cooling. The absorbance was measured at 416 nm with a UV Visible spectrophotometer (Shimadzu UV-1800 spectrophotometer, Japan). The inhibition (%) of protein denaturation was determined as follows[47].

$$\text{Protein denaturation inhibition } (\%) = \frac{(\text{Abs of test solution} - \text{Abs of product control})}{\text{Abs of test control}} \text{x } 100$$

2.8. Determination of antibacterial activity

Stock suspensions of *Staphylococcus aureus* ATCC 6538 strain were prepared by dispersing appropriate amounts of the bacterial culture (up to 5 %) in 5 mL of dimethyl sulfoxide (DMSO), generating a series of progressive dilutions ranging from 1250 to 9.8 μg/mL. The bacterial density was standardized using the McFarland method, following the guidelines of the National Committee for Clinical Laboratory Standards [48,49]. One aliquot (50 μL) of each bacterial suspension was added to the extract containing vesicles (10 mg/mL extract concentration), as well as to individual solutions of camphor and thymol (10 mg/mL each), to reach different concentrations of *Staphylococcus aureus* from 1 to 5 × 10^6 colony-forming units/mL. Test tubes were incubated at 37 °C for 24 h, after which bacterial growth was evaluated by measuring turbidity.

The bacterial suspension diluted in culture medium without any active compound served as the negative control, whereas the one containing moxifloxacin was used as the positive control.

2.9. In vitro studies with cells

Human lung adenocarcinoma epithelial cells (A549) were cultured in F-12K medium enriched with 10 % (v/v) foetal bovine serum, 1 % penicillin and streptomycin, and kept at 37 °C, 90 % humidity and 5 % CO_2; the cystic fibrosis (CuFi-1) cell line was cultivated in the same conditions but without serum. Prior to the experiment, CuFi-1 cell culture flasks were pre-coated for 18 h with a solution of type IV human placental collagen (60 μg/mL), then air-dried and washed 2–3 times with the medium to promote cell adhesion and growth.

These two cell lines were chosen for their wide application in respiratory research; CuFi-1 mimics nasal epithelial activity, and A549 acts as a model for alveolar epithelium, both ideal for biocompatibility and antioxidant investigations.

2.9.1. Biocompatibility and protective effect against oxidative stress of extract-loaded vesicles

1×10^4 cells were transferred into 96-well plates for 24 h and then treated for 48 h with extract in dispersion or loaded into vesicles properly diluted with the medium to obtain four different concentrations (10, 1, 0.1, 0.01 μg/mL of extract). Afterwards, 100 μL of Cell Counting Kit-8 (10 % final concentration) was added to each well. Plates were incubated for 3 h, and their optical density was measured at 570 nm with a microplate reader (Synergy 4 Reader, BioTek Instruments, AHSI S.p.A, Bernareggio, Italy). Analyses were carried out in triplicate. Cell viability was expressed as a percentage relative to the untreated control, which was considered 100 % viable.

To assess the protective effect of vesicles against hydrogen peroxide-induced cellular damage and death, cells were seeded at a density of 1×10^4 cells/well in 96-well plates and incubated for 24 h. The extract, either in dispersion or loaded in vesicles, was properly diluted with medium to reach two different concentrations (0.1 and 0.01 μg/mL), and added to cells that were stressed with hydrogen peroxide (1:30,000 v/v dilution). After 4 h of incubation, cells were washed with fresh medium, and their viability was measured using the Cell Counting Kit-8 as described above.

2.10. In vivo evaluation of antibacterial efficacy of vesicles

Staphylococcus aureus was selected as a representative strain and model microorganism for evaluating the antibacterial efficacy of the nasal formulation *in vivo*, considering that it is a common nasal colonizer and a frequent cause of respiratory infections [50]. BALB male mice aged 6–9 weeks were used. The study protocol was approved by the Ethical Committee for Research on Animals at Al-Ahliyya Amman University (SR-F17-14-003-Eng, Rev. a; Ref.: 07/24/2021–2022; Date: February 22, 2022), and conducted in accordance with national and international guidelines for the care and use of laboratory animals (ARRIVE guidelines, NIH Guide for the Care and Use of Laboratory Animals). The non-infected and untreated group served as a positive control. The infected and untreated group was used as a negative control. To infect mice, *Staphylococcus aureus* was directly applied to their nose using a nasal swab under a vertical biosafety laminar airflow. At day 1, 2, 3, 4, and 5 after the infection, vesicles (1 mL) were administered by inhalation to infected mice. At day 5, the mucosa of animals was taken with a swab. To avoid contamination, the bacterial strains were moved to aseptic Petri plates. To enable the growth of bacteria, Petri dishes with an appropriate nutritional agar medium were incubated at 37 °C for 24 h. Following the incubation, the resulting colonies were visually checked and counted by categorizing each individual colony. The data was determined as colony forming units (CFU) per plate to quantify bacterial growth accurately.

Table 1
Total phenolic content and antioxidant activity of *Obeidi* extract measured with DPPH, CUPRAC, and FRAP.

Analysis	Concentration
Total phenolic content	317.6 ± 2.1 mg of Gallic acid equivalents/g of extract
DPPH	621.9 ± 2.8 μg of Trolox equivalents/g of extract
CUPRAC	3.4 ± 0.3 mM of TEAC
FRAP	2.3 ± 0.1 mM of Iron II

2.11. Statistical analysis

All data were reported as average values and standard deviation and were calculated using GraphPad Prism 8 Statistical software. When p was >0.05, the differences were considered non-significant. Values were analysed using the two-way ANOVA test and Student t-test.

3. Results

3.1. Characterization of grape extract

The extract obtained from the seeds separated from the *Obeidi* grape pomace was deeply characterized (Table 1). An estimation of the total antioxidant activity of the extract was measured using different chromogenic redox reagents to evaluate its overall potential in different media. The total phenolic content of the extract was 317.6 ± 2.1 mg of gallic acid equivalents/g of extract. These phenolic compounds had a good ability to scavenge free radicals in methanol, donating an electron or hydrogen atom, as the amount of Trolox equivalents/g of extract was 621.9 ± 2.8 [36]. The antioxidant capacity of the extract was also evaluated using CUPRAC reagent (3.4 ± 0.3 mM of TEAC) and FRAP (2.3 ± 0.1 mM of Iron II), displaying its capacity for lowering metal ions. Findings have been reported as a function of standard compounds (Trolox and Fe^{2+} equivalents, respectively) [51].

The FTIR spectra of the extract had an O-H band ranging from 3500 cm^{-1} to 2700 cm^{-1}, as well as a C-H band extending between 3050 cm^{-1} (asymmetric stretch) and 2850 cm^{-1} (symmetric stretch). Furthermore, C=C double-bond stretching was present at 1600 and 1510 cm^{-1} and substantial C-O stretching at 1030 cm^{-1}. The 1450 cm^{-1} band is a C-H asymmetric distortion (Fig. 1a). Thus, the peaks of the spectra corroborate the presence of different organic molecules with unsaturated bounds and hydroxylic groups.

The main components were separated and identified by LC-MS/MS (Fig. 1b). The most evident peaks were those of sugars such as fructose and sucrose, alongside with organic acids (lactic acid, malic acid, palmitic acid) and glycerol. No signs of molecule degradation were detected in the chromatogram. The peaks of phenols were less evident, and their amount were quantified (Fig. 1c). Among these, gallic acid was the most abundant (19.40 μg/g of extract), followed by caffeic acid ester (8.10 μg/g of extract), resveratrol (4.73 μg/g of extract), and apigenin (4.70 μg/g of extract).

3.2. Characterization of vesicles

Considering the promising content of extract, it was co-loaded with camphor and thymol in PG-PEVs and carrageenan PG-PEVs. The actual formation of vesicles and their morphology and structure was observed by cryo-TEM (Fig. 2). Irrespective of the presence of carrageenan, both samples were mostly formed by unilamellar and spherical vesicles. Inside some vesicles, tangled lamellae were observed, probably because of the presence of multiple active components that interact with the phospholipids generating these special internal structures, as previously reported by Perra ***et al.*** [52].

Mean diameter, polydispersity, zeta potential and entrapment efficiency of the vesicles were measured (Table 2). The average diameter of

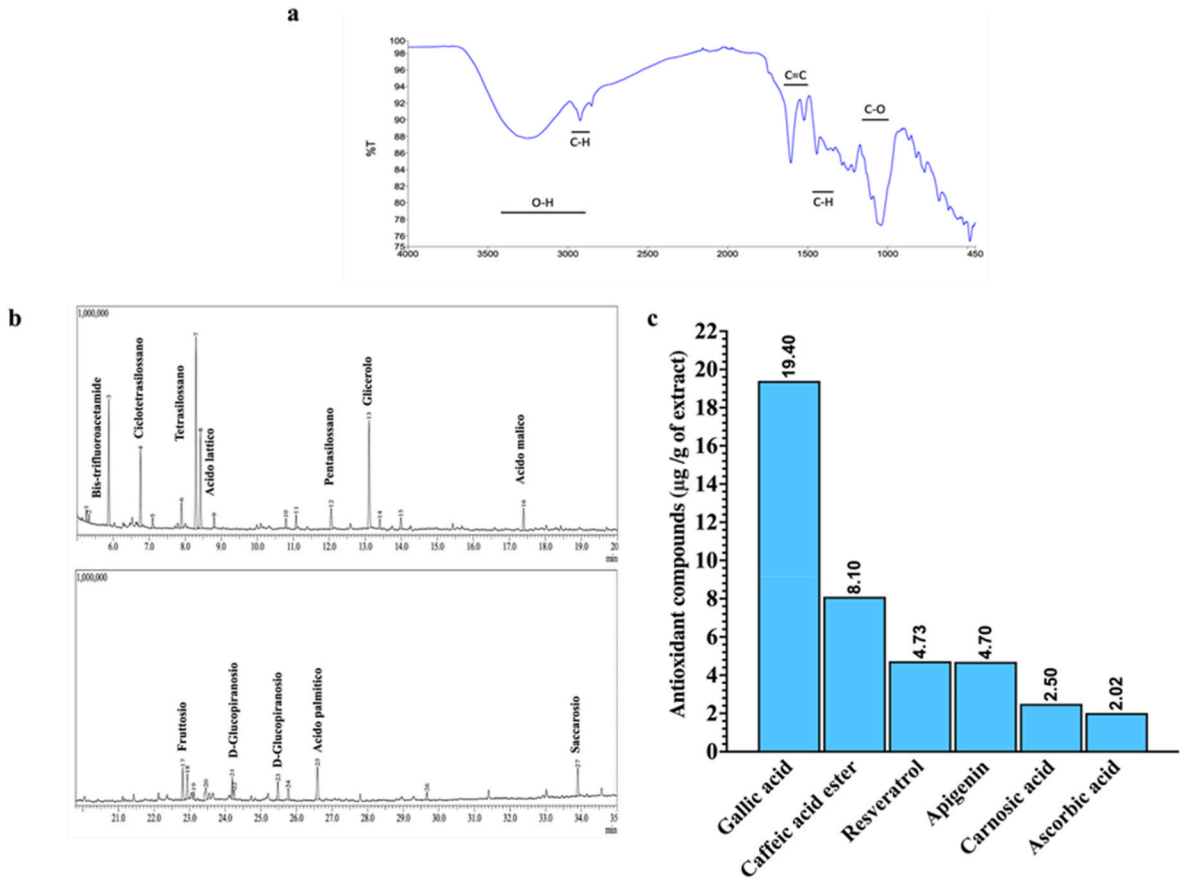

Fig. 1. (**a**) FTIR spectra of the extract obtained reporting wavelengths as a function of the transmittance. (**b**) chromatogram displaying the most abundant peaks of the extract (full list in supplementary material SM1). (**c**) amount of main antioxidant compounds (mg/g of extract) identified in the extract by LC-MS (see the full list in supplementary material SM2).

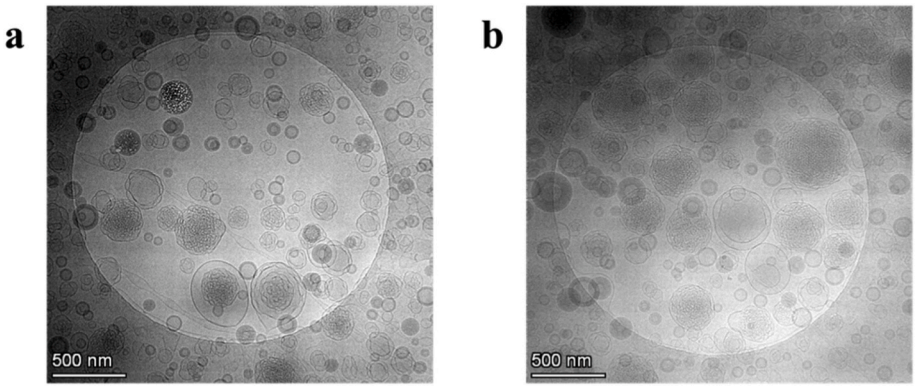

Fig. 2. Cryo-TEM images of extract-loaded PG-PEVs (**a**) and carrageenan PG-PEVs (**b**).

Table 2
Mean diameter (MD), polydispersity index (PI), zeta potential (ZP), entrapment efficiency (EE), and antioxidant activity (AA) of extract-loaded PG-PEVs and carrageenan PG-PEVs. Mean values ± standard deviations are reported.

	Mean diameter (nm)	Polydispersity index	Zeta potential (mV)	Encapsulation efficiency (%)	Antioxidant activity (%)
PG-PEVs	177 ± 5	0.252	−63 ± 4	90 ± 1	85 ± 1
Carrageenan PG-PEVs	194 ± 6	0.265	−60 ± 3	87 ± 1	88 ± 1

PG-PEVs was ~177 nm and that of carrageenan PG-PEVs was slightly bigger (~194 nm). Both formulations were homogeneously dispersed as the polydispersity index ranged from 0.25 to 0.27. The zeta potential was substantially negative, due to the negative charge of phosphatidylcholine and the presence of propylene glycol [53,54]. Vesicles were capable of loading and retaining a high amount of extract (~87–90 %), irrespective of the presence of carrageenan in the formulation, without interfering with its antioxidant activity, which remained

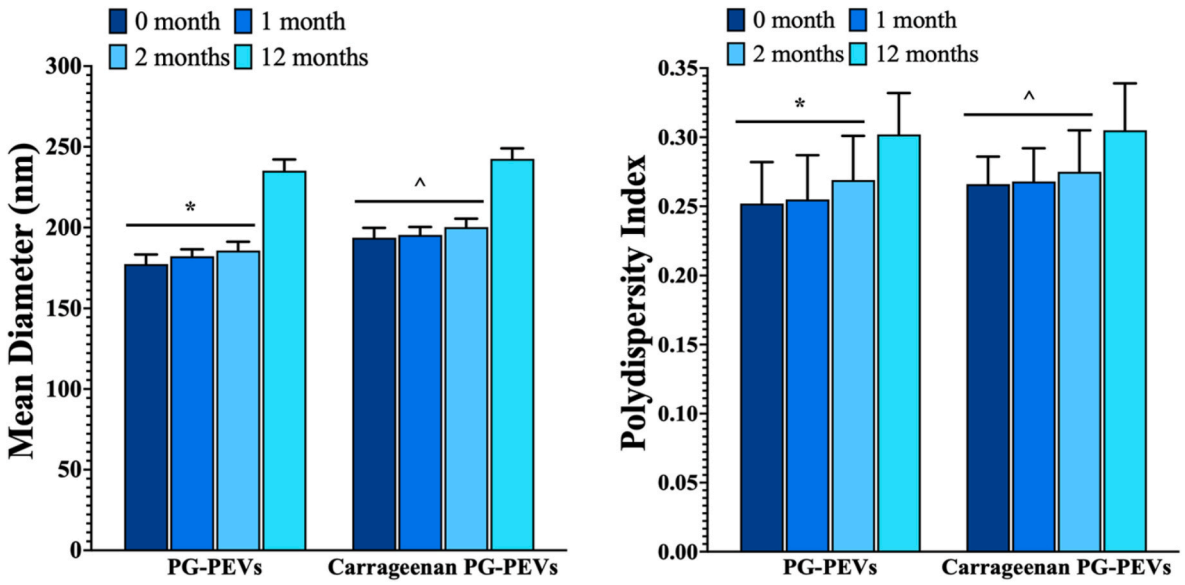

Fig. 3. Mean diameter and polydispersity index of extract-loaded PG-PEVs and carrageenan PG-PEVs measured for up to 12 months. Mean values ± standard deviations (bars) are reported. Symbols indicate values that are statistically not different ($p>0.05$).

Table 3
Size distribution of droplets generated by extract-loaded PG-PEVs and carrageenan PG-PEVs sprayed 4 cm and 7 cm from the laser beam. Dv(10), Dv(50) and Dv(90) indicate the size of 10 %, 50 % and 90 % of droplets. Mean values ± standard deviations (bars) are reported.

PG-PEVs				Carrageenan PG-PEVs			
Distance: 4 cm		Distance: 7 cm		Distance: 4 cm		Distance: 7 cm	
Dv(10)	50 μm ± 3.5	**Dv(10)**	55 μm ± 3.9	**Dv(10)**	49 μm ± 3.2	**Dv(10)**	52 μm ± 3.6
Dv(50)	70 μm ± 4.9	**Dv(50)**	65 μm ± 4.6	**Dv(50)**	73 μm ± 5.1	**Dv(50)**	69 μm ± 4.8
Dv(90)	96 μm ± 6.7	**Dv(90)**	106 μm ± 7.4	**Dv(90)**	118 μm ± 8.1	**Dv(90)**	135 μm ± 8.5
Span	0.724 ± 0.05	**Span**	0.823 ± 0.06	**Span**	0.467 ± 0.03	**Span**	0.421 ± 0.03

high (~85–88 %).

To evaluate the stability of vesicles in dispersion, their mean diameter and polydispersity index were measured at scheduled time points up to 12 months, by means of dynamic light scattering using the Zetasizer Ultra (Fig. 3). The mean diameter and the polydispersity index of both samples remained unchanged up to 2 months and slightly increased at 12 months. The diameter reached ~240 nm, and the polydispersity index was ~0.3 at the end of the evaluation, probably due to an arrangement of the assembling structure, which significantly changed the curvature radius that becoming smaller lead to an increased vesicle size.

3.3. Determination of droplet size generated by vesicle spray

To prevent inhalation into the lungs of sprayed formulations and allow for localised deposition in the nose, the Food and Drug Administration (FDA) and European Medicines Agency (EMA) recommend demonstrating that the vast majority of the droplets are larger than 10 μm [55]. Thus, both PG-PEVs and carrageenan PG-PEVS were sprayed with the Nasonex device, and the size of the generated droplets was measured via laser diffraction (Table 3). In compliance with the recommendations of the FDA, measures were taken at 4 cm and 7 cm from the laser beam (distance measured from the nozzle exit), with the pump apparatus angled at 45° [56]. The 10th percentile (Dv10) showed droplets of ~50 μm in diameter, regardless of the distance (4 or 7 cm) and whether the formulation contained carrageenan (carrageenan PG-PEVs) or not (PG-PEVs). Similarly, the median diameter (Dv50) was ~70 μm across all conditions, reflecting a high degree of homogeneity, as confirmed by the extremely narrow span values (~1). Lastly, 90 % of

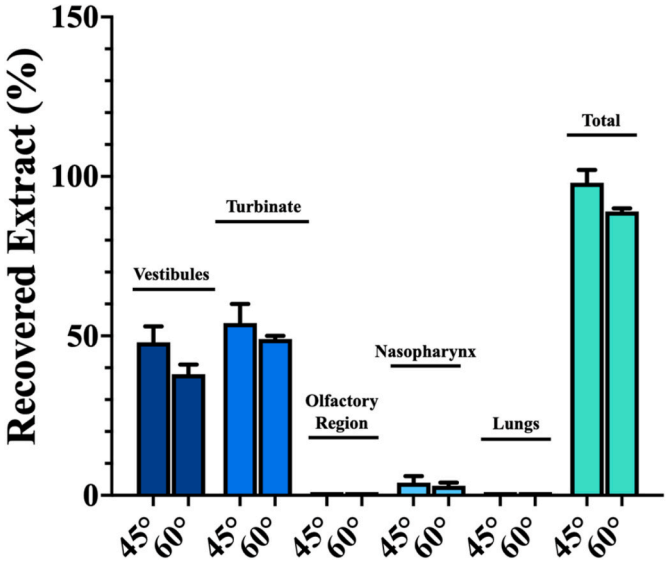

Fig. 4. Amount of recovered extract (%) delivered by PG-PEVs and carrageenan PG-PEVs and deposited in the different regions of the Alberta Idealized Nasal Inlet (vestibules, turbinates, olfactory region, and nasopharynx) coupled with the Next Generation Impactor (lungs).

droplets (Dv90) generated by carrageenan PG-PEVs were sized ~118 μm at 4 cm and ~135 μm at 7 cm, whereas those of PG-PEVs were sized ~96 μm at 4 cm and ~106 μm at 7 cm. Therefore, on the whole, these results indicate that the majority of droplets were well above 10 μm, as recommended by the FDA and EMA, suggesting that they would likely deposit within the nasal cavity after using the device.

3.4. Regional droplet deposition

Using the same device as in 3.3, the formulations were sprayed into the Alberta Idealized Nasal Inlet, coupled with the Next Generation Impactor, and the percentage of extract was measured to assess regional deposition (Fig. 4). The device was positioned at 45° and 60° relative to the realistic nasal replica. Irrespective of the applied angle and vesicle formulation, the payloads did not reach the lung-mimicking region (Next Generation Impactor), and their primary deposition occurred in the regions mimicking the vestibule and turbinate area. However, the percentage of extract recovered after deposition in the nasal replica was higher when the device was actuated at 45° rather than at 60°, particularly in the turbinate region. The turbinates divide the posterior nasal cavity into narrow passages; the space between the turbinates and the nasal wall is known as the meatus, where the sinus openings are located [57]. Consequently, the 45° angle appeared to be the most effective, allowing for the highest deposition (~50 %) in the target region (i.e., the turbinate), an area often implicated in upper airway inflammatory conditions such as rhinitis, sinusitis, and rhinosinusitis.

3.5. Biocompatibility and protective effect against oxidative stress of vesicles

A549 cells, derived from human lung epithelial tissue, are often employed as a broad respiratory epithelial model due to their simplicity in culture and mediator expression [58]. CuFi-1 cells, derived from a cystic fibrosis bronchial epithelial cell, have properties comparable to those of nasal epithelial cells, including the generation of mucus and oxidative stress responses. Altogether, these two cell models enabled the evaluation of biocompatibility and the ability of formulations to protect against hydrogen peroxide-induced oxidative stress.

When both cell lines were incubated with the extract, camphor, and thymol (at different dilutions), either in dispersion or loaded into vesicles, their viability decreased with increasing concentration. In the case of A549 cells (Fig. 5a), the incubation with the extract, camphor, and thymol in dispersion at the highest concentration (10 μg/mL of extract) resulted in a reduction of cell viability to ~42 %. By contrast, viability increased up to ~100 % when using the lowest concentration (0.01 μg/mL of extract). Incubating the same cells with extract, camphor, and thymol loaded PG-PEVs the viability was ~60 % when exposed to the highest concentration (10 μg/mL of extract) and ~117 % at the lowest concentration (0.01 μg/mL of extract). Using the extract, camphor, and thymol loaded carrageenan PG-PEVs cell viability was comparable at the highest concentration but at the lowest concentration (0.01 μg/mL of extract) it increased up to ~134 %. Carrageenan alone was tested as well to evaluate its effect on cell viability, and even in this case, biocompatibility was strictly dependent on the concentration tested, with the lowest concentration being the safest one (~93 % viability). CuFi-1 cells (Fig. 5b) were less sensitive to the extract, camphor, and thymol, since when they were used at the highest concentration (10 μg/mL of extract), cell viability was ~60 % and increased up to ~110 % using the lowest concentration (0.01 μg/mL of extract). However, when loaded in PG-PEVs, and especially in carrageenan PG-PEVs, cell viability was even higher (~139 % and ~160 %, at 0.01 μg/mL). Nonetheless, at the highest concentration (10 μg/mL), carrageenan PG-PEVs were more tolerated than PG-PEVs by CuFi-1 cells as evidenced by the viability (~68 % vs ~79 %, respectively). This effect may be partially attributed to the presence of carrageenan, which also showed good compatibility alone (~102 %).

When cells were stressed with hydrogen peroxide and not protected with formulations, the viability of A549 was ~59 % and that of CuFi-1 was ~57 % (Fig. 6a and b, respectively). Conversely, the exposure to the extract, camphor, and thymol loaded in vesicles at the lowest and non-toxic concentration (0.01 μg/mL of extract) increased cell viability thanks to their ability to counteract the damages caused by hydrogen peroxide. This increase was affected by cell type, formulation, and concentration tested. Specifically, the viability of A549 treated with extract, camphor, and thymol loaded PG-PEVs was ~89 %, and with extract, camphor, and thymol loaded carrageenan PG-PEVs was ~98 %

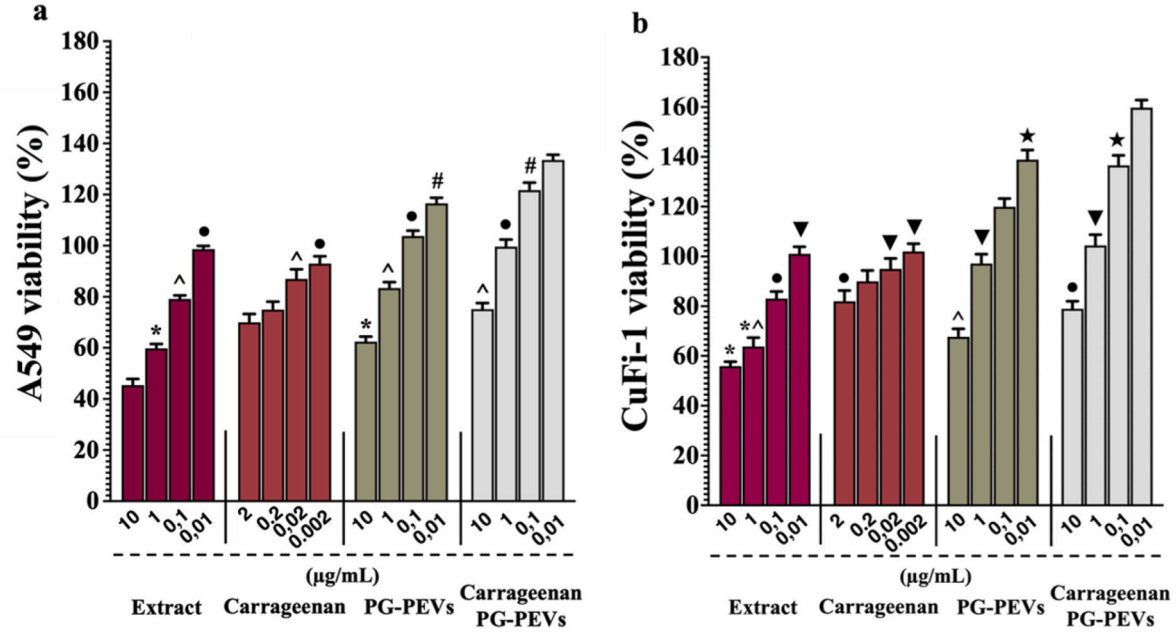

Fig. 5. Viability (%) of (**a**) A549 epithelial cells and (**b**) CuFi-1 cystic fibrosis cells incubated for 48 h with extract, camphor, and thymol in aqueous dispersion or loaded in PG-PEVs and carrageenan PG-PEVs. Data (bars) are reported as mean values ± standard deviations of cell viability, expressed as the percentage of control (untreated cells, 100 %). Identical symbols represent values with no statistically significant differences ($p>0.05$).

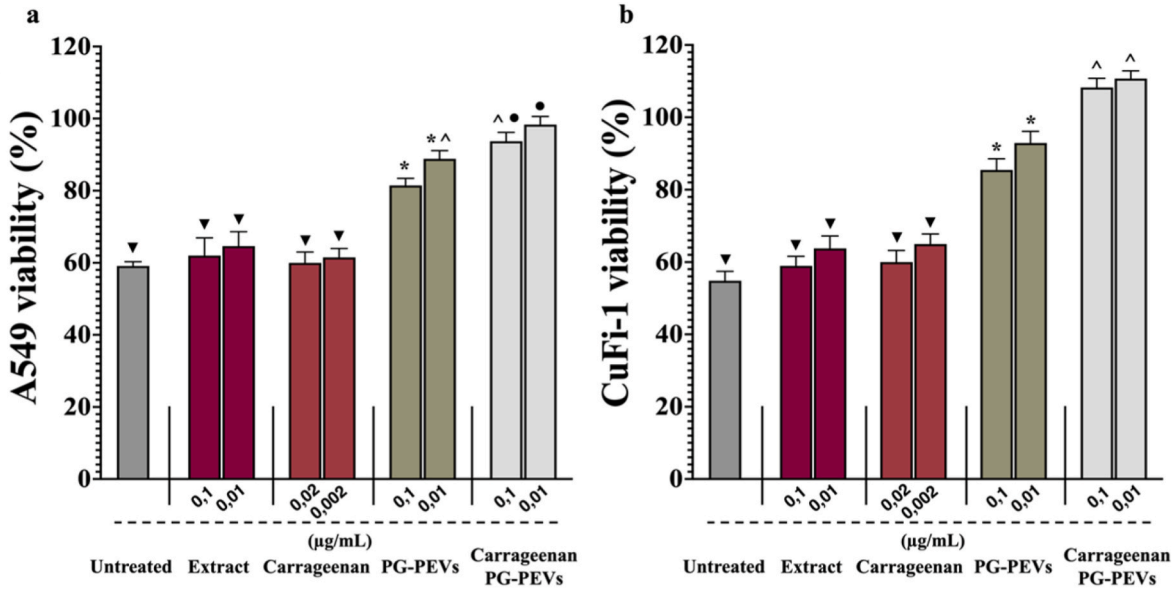

Fig. 6. Viability (%) of (**a**) A549 epithelial cells **b**) CuFi-1 cystic fibrosis cells stressed with hydrogen peroxide and treated with the extract, camphor, and thymol in aqueous dispersion or loaded in PG-PEVs carrageenan PG-PEVs and. Data are reported as mean values ± standard deviations of cell viability, expressed as the percentage of control (untreated cells, 100 %). Identical symbols represent values with no statistically significant differences ($p>0.05$).

(Fig. 6a). The viability of CuFi-1 cells treated with extract, camphor, and thymol loaded PG-PEVs was ~93 % and that of Cu-Fi-1 treated with extract, camphor, and thymol loaded carrageenan PG-PEVs was ~110 % (Fig. 6b). In both cases, the promising results are likely due to the synergistic effects of various components and the benefits deriving from encapsulation, as the viability of cells stressed with hydrogen peroxide and treated with carrageenan alone was sensibly lower (62 % for A549 cells and ~65 % for CuFi-1 cells, Fig. 6a and b, respectively) than that of loaded PG-PEVs and carrageenan PG-PEVs. Overall results seem to confirm the ability of vesicles to interact with cells, promoting the internalization of the payload and the exertion of its activity.

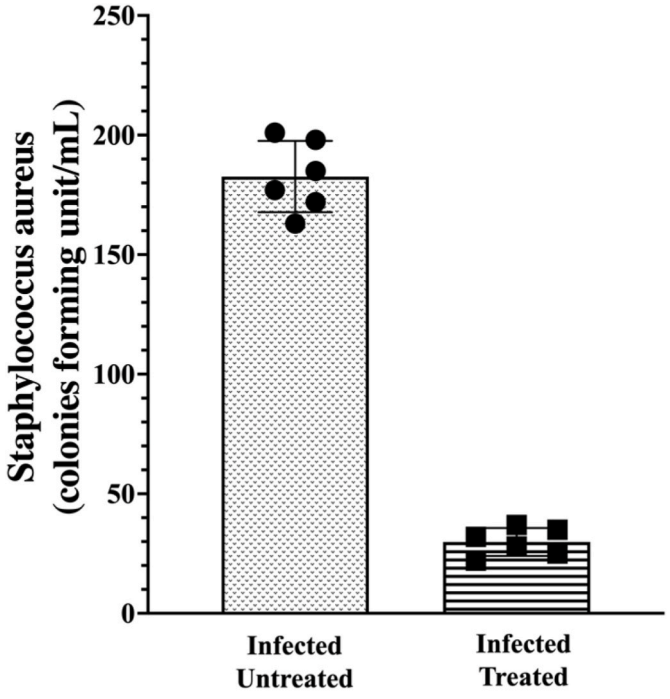

Fig. 7. Number of colonies of *Staphylococcus aureus* found in the mice infected and untreated or infected and treated with extract, thymol, and camphor loaded in carrageenan PG-PEVs. Mean values ± standard deviations are reported (n = 6).

3.6. Protein denaturation inhibition and antibacterial activity

As a measure of the potential anti-inflammatory activity, the ability of formulations to inhibit protein denaturation was evaluated. The extract, camphor, and thymol loaded in PG-PEVs and carrageenan PG-PEVs, were able to inhibit the protein denaturation up to ~90 % irrespective of the vesicle composition, suggesting their potential ability to reduce the release of pro-inflammatory mediators (i.e., cytokines, ROS).

The *in vitro* antibacterial activity of the formulations showed an IC_{50} of approximately 468.75 µg/mL, regardless of carrageenan addition. These results confirmed that the combination of the active components together with their incorporation into phospholipid vesicles either enriched or not with carrageenan may be responsible of the promising outcomes obtained *in vitro*, suggesting a synergistic action capable of improving antioxidant, anti-inflammatory and antibacterial activities.

3.7. In vivo antibacterial efficacy

Considering the ability of extract, thymol, and camphor loaded carrageenan PG-PEVs to ensure a better protection against oxidative stress, they were further studied *in vivo*. The mice infected with *Staphylococcus aureus* were treated via inhalation with the formulation, and its ability to counteract the pathogen proliferation was assayed (Fig. 7). After being infected for 5 days, the number of *Staphylococcus aureus* colonies were ~180 CFU/mL, confirming the persistence and robustness of the infection model. At day 5, after the inhalation of formulation, the number of colonies was reduced to ~30 CFU/mL, indicating an important antibacterial effect provided by the treatment and probably due to the synergic effect of camphor, thymol, and carrageenan [59]. No signs of local toxicity, irritation, or inflammation were observed in the nasal mucosa of mice after the treatment period. All treated animals exhibited normal behavior with no visible redness, swelling, or nasal discharge, indicating a significant antibacterial effect likely due to the synergistic action of camphor, thymol, and carrageenan. Both positive (healthy, not infected mice) and negative (infected and untreated mice) control groups were included in this study.

4. Discussion

Liposomes are composed of phospholipids, which also approximately constitute 75 % of the natural surfactant layer of the nasal mucosa [60]. Thanks to this unique composition and their efficient carrier performances, these vesicles offer a dual advantage in nasal delivery, facilitating the localized release of loaded molecules and acting themselves as moisturizing agents that improve the physiological homeostasis of mucosae. For this reason, liposomes have been widely used on the inflamed nasal mucosa, and some formulations are commercially available on the market [61]. Building on the current state of the art, this study focused on the development of modified phospholipid vesicles, termed PG-PEVs, composed of phospholipids, propylene glycol, and carrageenan, a natural gelling agent capable of forming a protective barrier over the nasal mucosa. In a previous study, it also prevented infectious viruses from binding to the mucosal cells, thus improving the treatment and prevention of Coronavirus disease [62]. In this research, it enhanced vesicle stability and contributed to repressing the spread of *Staphylococcus aureus*. The resulting carriers (PG-PEVs and carrageenan PG-PEVs) were used to deliver intranasally the extract obtained from *Obeidi* grape seeds, which due to its high content of phenols (e.g., gallic acid, resveratrol, etc.), was strongly antioxidant and able to protect the cells from oxidative damage and inflammation, in agreement with the *in vitro* studies performed by Gibis ***et al.*** and Delgado Adámez ***et al.*** [63,64]. In addition to their antioxidant properties, several authors have demonstrated that these compounds also possess antimicrobial properties. For instance, Francioso ***et al.*** reported that resveratrol, when administered in combination with a carboxymethyl-β-glucan solution as an aerosol, significantly reduced the spread of rhinoviruses in human nasal epithelial tissues [65]. Similarly, Esposito ***et al.*** demonstrated that a nasal spray formulation of propolis enriched with polyphenols effectively alleviated symptoms related to bacterial infections, promoting rapid recovery and reducing the need for acute treatments [66]. To leverage the intrinsic properties of the extract and improve the antimicrobial activity of the formulations, two additional antimicrobial compounds – camphor and thymol – were co-loaded [67]. The versatility of both PG-PEVs and carrageenan PG-PEVs enabled the simultaneous loading of three different and complementary payloads (extract, camphor, and thymol). The resulting vesicles were sized ~177 and ~194 nm, respectively. Such small sizes are considered suitable for nasal delivery, as they allow for bypassing the mucosal barrier and enhancing local absorption in the nasal cavity [68,69]. In addition, they both displayed a monodisperse size distribution and a negative surface charge, in line with findings reported by Manca ***et al.***, who observed similar characteristics when encapsulating a grape pomace extract in phospholipid vesicles [70]. After 12 months of storage, formulation size slightly increased (10 %) and the samples became somewhat polydispersed, confirming that some internal but not significant rearrangements occurred.

Foreseeing a potential nasal administration of the formulations, they were loaded into a readily available commercial device (i.e., Nasonex). The spraying device produces a conical shape of aerosolized droplets, which based on their size would deposit in the respiratory tract at different levels. Usually, droplets larger than 10 μm can reach the nasal cavity, while those larger than 120 μm tend to settle in the anterior region of the nose, creating a regional impact [71,72]. Therefore, the sprayability of vesicles was also assessed by quantifying the mean diameter of droplets formed after actuation of the device [73,74]. 50 % of droplets were sized ≤50 μm, confirming their suitability for nasal spraying and potential deposition in the nasal cavity. These results were further supported by the quantity of loaded extract recovered in each stage of a realistic nasal replica. The main fraction was recovered in the turbinates, corresponding to the posterior nasal cavity, where they can exert their action against local allergies, and congestion [75]. No extract was found in the deeper stages, interrelated to deeper airways (i.e., lungs), similar to the findings previously published by Seifelnasr ***et al.*** [76].

In vitro and *in vivo* studies followed these encouraging results. First, grape seed extract, camphor, and thymol loaded into PG-PEVs and carrageenan PG-PEVs synergistically inhibited protein denaturation by 90 %, confirming a significant anti-inflammatory potential as described elsewhere [77]. Then, the loaded PG-PEVs and carrageenan PG-PEVs demonstrated good biocompatibility and antioxidant protection against hydrogen peroxide-induced oxidative stress *in vitro*, on A549 and CuFi-1 cell lines. At the highest concentration of 10 μg/mL of extract, a slight toxicity was detected (~ 60 % viability), but at lower concentrations (0.1 and 0.01 μg/mL), cell viability increased significantly reaching values ≥ 100 %. These results are promising, especially given the complex structure of the nose that, while offering advantages such as bypassing first-pass metabolism and potentially rapid onset of action, can face challenges with drug absorption due to factors like the nasal mucosa's structure and mucociliary clearance [78–80]. In this context, the amount of drug that may be absorbed upon nasal administration can be very low, approaching the lower concentrations tested *in vitro* with cells, thus suggesting that incorporation of payloads into vesicular formulations may ensure their effectiveness even at low concentrations, as previously demonstrated by other authors [78,81,82]. Notably, it was at these lower concentrations that the incorporated extract and molecules significantly improved the protection of A549 and CuFi-1 cells from the oxidative damage caused by hydrogen peroxide to a greater extent than their aqueous dispersion used as a reference. Considering these data and the sulfated polysaccharide nature of carrageenan, which possesses mucoadhesive properties useable to prolong the residence time of vesicles in the nasal cavity, carrageenan PG-PEVs were selected for the *in vivo* studies [83] Due to the synergism between extract, camphor, and thymol, the loaded carrageenan PG-PEVs sensibly reduced bacterial colonies of *Staphylococcus aureus* in the nasal cavity. Altogether, these findings underscore the potential effectiveness of this new natural formulation in managing nasal congestion, counteracting different factors such as mucosa dysbiosis, oxidative stress, inflammation, and infection.

5. Conclusions

This study demonstrated that the extract obtained from Obeidi pomace seeds can be effectively co-loaded with camphor and thymol into PG-PEVs, obtaining small, monodispersed, and negatively charged nanosystems suitable for nasal delivery. Further enrichment with carrageenan not only does not affect such properties but also provides synergistic anti-inflammatory and antibacterial effects on the nasal mucosa. The droplet size distribution and the deposition pattern following spraying suggest suitability for nasal delivery, with preferential accumulation in the posterior nasal cavity, where the combined activity of grape polyphenols, thymol, and camphor delivered by the formulations, especially those enriched with carrageenan, can represent a natural and local therapeutic approach for managing different nasal conditions such as rhinitis, sinusitis and rhinosinusitis.

Despite the promising results and the observed biological effects suggesting cooperative interaction among the active compounds, the present study does not include molecular or biochemical analyses to elucidate the exact mechanisms of action. Further research is needed to explore the specific intracellular pathways involved and to directly evaluate the effects of the formulations on mucociliary clearance, mucoadhesiveness, and their residence time within the nasal cavity.

CRediT authorship contribution statement

Rita Abi Rached: Writing – original draft, Data curation, Conceptualization. **Ashok K. Shakya:** Formal analysis, Data curation. **Maria Letizia Manca:** Writing – original draft, Supervision, Data curation, Conceptualization. **Matteo Aroffu:** Formal analysis, Data curation. **Fátima García-Villén:** Formal analysis, Data curation. **Joe A. Touma:**

Resources. **Xavier Fernàndez-Busquets:** Formal analysis, Data curation. **Marija Ivanov:** Formal analysis, Data curation. **Jose Luis Pedraz:** Formal analysis, Data curation. **Nicolas Louka:** Writing – original draft, Data curation, Conceptualization. **Richard G. Maroun:** Writing – original draft, Supervision, Data curation, Conceptualization. **Maria Manconi:** Writing – original draft, Supervision, Data curation, Conceptualization.

Funding

This research did not receive any specific grant from funding agencies in the public, commercial, or not-for-profit sectors.

Declaration of competing interest

The authors declare that they have no known competing financial interests or personal relationships that could have appeared to influence the work reported in this paper.

Acknowledgments

ISGlobal and IBEC are members of the CERCA Programme, *Generalitat de Catalunya*. We acknowledge support from the Spanish Ministry of Science, Innovation and Universities through the *"Centro de Excelencia Severo Ochoa 2019–2023"* Program (CEX2018-000806-S). This research is part of ISGlobal's Program on the Molecular Mechanisms of Malaria which is partially supported by the *Fundación Ramón Areces*. We also like to acknowledge the Deanship of Pharmacy, Al-Ahliyya Amman University, Amman, Jordan for conducting part of research work during the Erasmus Exchange program. Lastly, we thank the ICTS "NANBIOSIS" and the Drug Formulation Unit (U10) of the CIBER in Bioengineering, Biomaterials and Nanomedicine (CIBER-BBN), and consolidated groups (IT1448-22) at the University of Basque Country (UPV/EHU). This research was funded by the Ministry of Science, Technological Development and Innovations of the Republic of Serbia, grant numbers 451-03-66/2024-03/200007.

Appendix A. Supplementary data

Supplementary data to this article can be found online at https://doi.org/10.1016/j.jddst.2025.107342.

Data availability

The authors are unable or have chosen not to specify which data has been used.

References

[1] J.R. Harkema, S.A. Carey, J.G. Wagner, The nose revisited: a brief review of the comparative structure, function, and toxicologic pathology of the nasal epithelium, J. Toxicol. Pathol. 34 (2006) 252–269, https://doi.org/10.1080/01926230600713475.

[2] V.J. Feron, J.H.E. Arts, C.F. Kuper, P.J. Slootweg, R.A. Woutersen, Health risks associated with inhaled nasal toxicants, Critical Rev. Toxicol. 31 (3) (2001) 313–347, https://doi.org/10.1080/20014091111712.

[3] M. Hoggard, B.W. Mackenzie, R. Jain, M.W. Taylor, K. Biswas, R.G. Douglas, Chronic rhinosinusitis and the evolving understanding of microbial ecology in chronic inflammatory mucosal disease, J. Clin. Microbiol. Rev. 30 (2017) 321–348, https://doi.org/10.1128/CMR.00060-16.

[4] W.W. Stevens, R.J. Lee, R.P. Schleimer, N.A. Cohen, Chronic rhinosinusitis pathogenesis, J. Allergy Clin. Immunol. 136 (2015) 1442–1453, https://doi.org/10.1016/j.jaci.2015.10.009.

[5] L. Casettari, L. Illum, Chitosan in nasal delivery systems for therapeutic drugs, J. Contr. Release 190 (2014) 189–200, https://doi.org/10.1016/j.jconrel.2014.05.003.

[6] I. Zupanets, T. Zhulai, S. Shebeko, I. Otrishko, D. Hladkykh, Histomorphological study of a new nasal spray with anti-inflammatory properties efficacy in rabbits with rhinosinusitis, J. Med. Arch. 74 (2020) 8–13, https://doi.org/10.5455/medarh.2020.74.8-13.

[7] Y. Shu, H. Shen, M. Yao, J. Shen, G. Yang, H. Chen, Y. Tang, M. Ma, Metal protoporphyrin-induced self-assembly nanoprobe enabling precise tracking and antioxidant protection of stem cells for ischemic stroke therapy, Smart Med. 2 (2023), https://doi.org/10.1002/SMMD.20220037.

[8] X. Shen, Z. Zhang, C. Cheng, C. Liu, N. Ma, D. Sun, D. Li, C. Wang, Bone regeneration and antibacterial properties of calcium-phosphorus coatings induced by gentamicin-loaded polydopamine on magnesium alloys, Biomed. Technol. 5 (2024) 87–101, https://doi.org/10.1016/j.bmt.2023.06.002.

[9] P. Zhuang, W. Yang, Y. Chen, Y. Zhang, C. Leboucher, J.M. Rosenholm, H. Zhang, Biomaterials that passively and actively target macrophages promote the regeneration of injured tissues, Biomed. Technol. 8 (2024) 17–49, https://doi.org/10.1016/j.bmt.2024.09.005.

[10] Y. Sun, W. Zhang, Z. Luo, C. Zhu, Y. Zhang, Z. Shu, C. Shen, X. Yao, Y. Wang, X. Wang, ZnO-CuS/F127 hydrogels with multienzyme properties for implant-related infection therapy by inhibiting bacterial arginine biosynthesis and promoting tissue repair, Adv. Funct. Mater. 35 (2025), https://doi.org/10.1002/adfm.202415778.

[11] W. Wang, Y. Cui, X. Wei, Y. Zang, X. Chen, L. Cheng, X. Wang, $CuCo_2O_4$ nanoflowers with multiple enzyme activities for treating bacterium-infected wounds via cuproptosis-like death, ACS Nano 18 (2024) 15845–15863, https://doi.org/10.1021/acsnano.4c02825.

[12] Z. Hu, J. Shan, X. Jin, W. Sun, L. Cheng, X.-L. Chen, X. Wang, Nanoarchitectonics of *in situ* antibiotic-releasing acicular nanozymes for targeting and inducing cuproptosis-like death to eliminate drug-resistant bacteria, ACS Nano 18 (2024) 24327–24349, https://doi.org/10.1021/acsnano.4c06565.

[13] M.S. Taha, S. Kutlehria, A. D'Souza, B.S. Bleier, M.M. Amiji, Topical administration of verapamil in poly(ethylene glycol)-modified liposomes for enhanced sinonasal tissue residence in chronic rhinosinusitis: ex vivo and in vivo evaluations, J. Molecular Pharm. 20 (2023) 1729–1736, https://doi.org/10.1021/acs.molpharmaceut.2c00943.

[14] F. Laffleur, N. Hörmann, R. Gust, A. Ganner, Synthesis, characterization and evaluation of hyaluronic acid-based polymers for nasal delivery, Int. J. Pharm. 631 (2023) 122496, https://doi.org/10.1016/j.ijpharm.2022.122496.

[15] E. Casula, M.L. Manca, M. Perra, J.L. Pedraz, T.B. Lopez-Mendez, A. Lozano, E. Calvo, M. Zaru, M. Manconi, Nasal spray formulations based on combined hyalurosomes and glycerosomes loading Zingiber officinalis extract as green and natural strategy for the treatment of rhinitis and rhinosinusitis, J. Antioxidants 10 (2021) 1109, https://doi.org/10.3390/antiox10071109.

[16] E. Casula, M. Manconi, J. Vázquez, T. Lopez-Mendez, J. Pedraz, E. Calvo, A. Lozano, M. Zaru, A. Ascenso, M. Manca, Design of a nasal spray based on Cardiospermum halicacabum extract loaded in phospholipid vesicles enriched with gelatin or chondroitin sulfate, Molecules 26 (2021) 6670, https://doi.org/10.3390/molecules26216670.

[17] M. Manconi, C. Sinico, A.M. Fadda, Penetration enhancer-containing vesicles for cutaneous drug delivery, in: Percutaneous Penetration Enhancers Chemical Methods in Penetration Enhancement: Nanocarriers, Springer Berlin Heidelberg, 2016, pp. 93–110, https://doi.org/10.1007/978-3-662-47862-2_6.

[18] M. Chessa, C. Caddeo, D. Valenti, M. Manconi, C. Sinico, A.M. Fadda, Effect of penetration enhancer containing vesicles on the percutaneous delivery of Quercetin through new born pig skin, Pharmaceutics 3 (2011) 497–509, https://doi.org/10.3390/pharmaceutics3030497.

[19] M. Manconi, C. Caddeo, C. Sinico, D. Valenti, M.C. Mostallino, G. Biggio, A. M. Fadda, Ex vivo skin delivery of diclofenac by transcutol containing liposomes and suggested mechanism of vesicle-skin interaction, Eur. J. Pharm. Biopharm. 78 (2011) 27–35. http://www.scopus.com/inward/record.url?eid=2-s2.0-79953161603&partnerID=40&md5=685b6bef9fb4e722517ea095c13a9517.

[20] M. Manconi, C. Caddeo, C. Sinico, D. Valenti, M.C. Mostallino, S. Lampis, M. Monduzzi, A.M. Fadda, Penetration enhancer-containing vesicles: composition dependence of structural features and skin penetration ability, Eur. J. Pharm. Biopharm. 82 (2012) 352–359, https://doi.org/10.1016/j.ejpb.2012.06.015.

[21] M. Ghadiri, P.M. Young, D. Traini, Strategies to enhance drug absorption via nasal and pulmonary routes, Pharmaceutics 11 (2019) 113, https://doi.org/10.3390/pharmaceutics11030113.

[22] M.L. Manca, M. Manconi, A.M. Falchi, I. Castangia, D. Valenti, S. Lampis, A. M. Fadda, Close-packed vesicles for diclofenac skin delivery and fibroblast targeting, Colloids Surf. B Biointerfaces 111 (2013) 609–617, https://doi.org/10.1016/j.colsurfb.2013.07.014.

[23] C. Wang, Y. You, W. Huang, J. Zhan, The high-value and sustainable utilization of grape pomace: a review, J. Food Chem. 24 (2024) 101845, https://doi.org/10.1016/j.fochx.2024.101845.

[24] T.O.X. Machado, I. Portugal, H. de A.C. Kodel, D. Droppa-Almeida, M. Dos Santos Lima, F. Fathi, M.B.P.P. Oliveira, R.L.C. de Albuquerque-Júnior, C. Dariva, E. B. Souto, Therapeutic potential of grape pomace extracts: a review of scientific evidence, J. Food Biosci. 60 (2024) 104210, https://doi.org/10.1016/j.fbio.2024.104210.

[25] M.S. Dopico-García, A. Fique, L. Guerra, J.M. Afonso, O. Pereira, P. Valentão, P. B. Andrade, R.M. Seabra, Principal components of phenolics to characterize red Vinho Verde grapes: anthocyanins or non-coloured compounds? Talanta 75 (2008) 1190–1202, https://doi.org/10.1016/j.talanta.2008.01.012.

[26] C.G. Fraga, K.D. Croft, D.O. Kennedy, F.A. Tomás-Barberán, The effects of polyphenols and other bioactives on human health, Food Funct. 10 (2019) 514–528, https://doi.org/10.1039/c8fo01997e.

[27] V. Kapcsándi, E. Hanczné Lakatos, B. Sik, L.Á. Linka, R. Székelyhidi, Characterization of fatty acid, antioxidant, and polyphenol content of grape seed oil from different Vitis vinifera L. varieties, OCL - Oilseeds and fats, Crops Lipids 28 (2021) 30, https://doi.org/10.1051/ocl/2021017.

[28] I. Castangia, M.L. Manca, C. Caddeo, G. Bacchetta, R. Pons, D. Demurtas, O. Diez-Sales, A.M. Fadda, M. Manconi, Santosomes as natural and efficient carriers for the improvement of phycocyanin reepithelising ability in vitro and in vivo, Eur. J. Pharm. Biopharm. 103 (2016) 149–158, https://doi.org/10.1016/j.ejpb.2016.03.033.
[29] H. Natsheh, E. Touitou, Phospholipid vesicles for dermal/transdermal and nasal administration of active molecules: the effect of surfactants and alcohols on the fluidity of their lipid bilayers and penetration enhancement properties, Molecules 25 (2020) 2959, https://doi.org/10.3390/molecules25132959.
[30] N.L. Patil, H.S. Mahajan, American journal of advanced drug delivery American journal of advanced drug delivery, Am. J. Adv. Drug Deliv. 6 (2018), https://doi.org/10.21767/2321-547X.1000022. http://www.imedpub.com/advanced-drug-delivery/QuercetinLoadedNanostructuredLipidCarriersforNosetoBrainDelivery:InVitroandInVivoStudies.
[31] Y. Salem, H.N. Rajha, D. Franjieh, I. Hoss, M.L. Manca, M. Manconi, I. Castangia, M. Perra, R.G. Maroun, N. Louka, Stability and antioxidant activity of hydro-glyceric extracts obtained from different grape seed varieties incorporated in cosmetic creams, Antioxidants 11 (2022) 1348, https://doi.org/10.3390/antiox11071348.
[32] J. Shi, J. Yu, J.E. Pohorly, Y. Kakuda, Polyphenolics in grape seeds-biochemistry and functionality, J. Med. Food 6 (2003) 291–299.
[33] B. Antonić, S. Jančíková, D. Dordević, B. Tremlová, Grape pomace valorization: a systematic review and meta-analysis, Foods 9 (2020) 1627, https://doi.org/10.3390/foods9111627.
[34] Y. Salem, H.N. Rajha, L.A.M. van den Broek, C. Safi, A. Togtema, M. Manconi, M. L. Manca, E. Debs, Z. Hobaika, R.G. Maroun, N. Louka, Multi-step biomass fractionation of grape seeds from pomace, a zero-waste approach, Plants 11 (2022) 2831, https://doi.org/10.3390/plants11212831.
[35] R.M. L-R, Vernon L. Singleton, Rudolf Orthofer, Analysis of total phenols and other oxidation substrates and antioxidants by means of Folin-Ciocalteu Reagent, Sci. Hortic. 213 (2016) 281–286, https://doi.org/10.1016/j.scienta.2016.11.004.
[36] M.A. Gyamfi, M. Yonamine, Y. Aniya, Free-radical scavenging action of medicinal herbs from GhanaThonningia sanguinea on experimentally-induced liver injuries, Gen. Pharmacol. 32 (2000) 661–667, https://doi.org/10.1016/S0306-3623(98)00238-9.
[37] A.M. Abi-Khattar, H.N. Rajha, R.M. Abdel-Massih, R. Habchi, R.G. Maroun, E. Debs, N. Louka, "Intensification of Vaporization by Decompression to the Vacuum" (IVDV), a novel technology applied as a pretreatment to improve polyphenols extraction from olive leaves, Food Chem. 342 (2021) 128236, https://doi.org/10.1016/j.foodchem.2020.128236.
[38] Y. Mishra, H.I.M. Amin, V. Mishra, M. Vyas, P.K. Prabhakar, M. Gupta, R. Kanday, K. Sudhakar, S. Saini, A. Hromić-Jahjefendić, A.A.A. Aljabali, M. El-Tanani, Ã. Serrano-Aroca, H. Bakshi, M.M. Tambuwala, Application of nanotechnology to herbal antioxidants as improved phytomedicine: an expanding horizon, Biomed. Pharmacother. 153 (2022), https://doi.org/10.1016/j.biopha.2022.113413.
[39] R. Adams, Identification of Essential Oils Components by Gas Chromatography/Mass Spectroscopy, fifth ed., 2017. https://www.cabidigitallibrary.org/doi/full/10.5555/20083116584.
[40] O.D. Sparkman, Identification of essential oil components by gas chromatography/quadrupole mass spectroscopy Robert P. Adams, J. Am. Soc. Mass Spectrom. 16 (2005) 1902–1903, https://doi.org/10.1016/j.jasms.2005.07.008.
[41] W.E. Wallace, W. Ji, D.V. Tchekhovskoi, K.W. Phinney, S.E. Stein, Mass spectral library quality assurance by inter-library comparison, J. Am. Soc. Mass Spectrom. 28 (2017) 733–738, https://doi.org/10.1007/s13361-016-1589-4.
[42] M. Allaw, M.L. Manca, J.C. Gómez-Fernández, J.L. Pedraz, M.C. Terencio, O. D. Sales, A. Nacher, M. Manconi, Oleuropein multicompartment nanovesicles enriched with collagen as a natural strategy for the treatment of skin wounds connected with oxidative stress, Nanomedicine 16 (2021) 2363–2376, https://doi.org/10.2217/nnm-2021-0197.
[43] M. Manconi, M.L. Manca, E. Escribano-Ferrer, E.M. Coma-Cros, A. Biosca, E. Lantero, X. Fernàndez-Busquets, A.M. Fadda, C. Caddeo, Nanoformulation of curcumin-loaded eudragit-nutriosomes to counteract malaria infection by a dual strategy: improving antioxidant intestinal activity and systemic efficacy, Int. J. Pharm. 556 (2019), https://doi.org/10.1016/j.ijpharm.2018.11.073.
[44] J. Rissler, L. Asking, J.K. Dreyer, A methodology to study impactor particle reentrainment and a proposed stage coating for the NGI, J. Aerosol Med. Pulm. Drug Deliv. 22 (2009) 309–316, https://doi.org/10.1089/jamp.2008.0735.
[45] M. Manconi, M.L. Manca, D. Valenti, E. Escribano, H. Hillaireau, A.M. Fadda, E. Fattal, Chitosan and hyaluronan coated liposomes for pulmonary administration of curcumin, Int. J. Pharm. 525 (2017) 203–210, https://doi.org/10.1016/j.ijpharm.2017.04.044.
[46] J.Z. Chen, W.H. Finlay, A. Martin, In vitro regional deposition of nasal sprays in an idealized nasal inlet: Comparison with in vivo gamma scintigraphy, Pharm. Res. 39 (2022) 3021–3028, https://doi.org/10.1007/s11095-022-03388-7.
[47] B. Kar, R.B. Suresh Kumar, I. Karmakar, N. Dolai, A. Bala, U.K. Mazumder, P. K. Haldar, S. Lecturer, Antioxidant and in vitro anti-inflammatory activities of Mimusops elengi leaves Asian Pacific. www.elsevier.com/locate/apjtb, 2012.
[48] Y.M. Al-Hiari, I.S. Al-Mazari, A.K. Shakya, R.M. Darwish, R. Abu-Dahab, Synthesis and antibacterial properties of new 8-nitrofluoroquinolone derivatives, Molecules 12 (2007) 1240–1258, https://doi.org/10.3390/12061240.
[49] J.A. Kiehlbauch, G.E. Hannett, M. Salfinger, W. Archinal, C. Monserrat, C. Carlyn, Use of the National Committee for Clinical Laboratory Standards Guidelines for Disk Diffusion Susceptibility Testing in New York State Laboratories, 2000.
[50] B. Tilahun, A.C. Faust, P. McCorstin, A. Ortegon, Nasal colonization and lower respiratory tract infections with Methicillin-Resistant Staphylococcus aureus, Am. J. Crit. Care 24 (2015) 8–12, https://doi.org/10.4037/ajcc2015102.
[51] D. Villaño, M.S. Fernández-Pachón, M.L. Moyá, A.M. Troncoso, M.C. García-Parrilla, Radical scavenging ability of polyphenolic compounds towards DPPH free radical, Talanta 71 (2007) 230–235, https://doi.org/10.1016/j.talanta.2006.03.050.
[52] M. Perra, M.L. Manca, C.I.G. Tuberoso, C. Caddeo, F. Marongiu, J.E. Peris, G. Orrù, A. Ibba, X. Fernàndez-Busquets, S. Fattouch, G. Bacchetta, M. Manconi, A green and cost-effective approach for the efficient conversion of grape byproducts into innovative delivery systems tailored to ensure intestinal protection and gut microbiota fortification, Innov. Food Sci. Emerg. Technol. 80 (2022), https://doi.org/10.1016/j.ifset.2022.103103.
[53] D. Kawar, H. Abdelkader, Hyaluronic acid gel-core liposomes (hyaluosomes) enhance skin permeation of ketoprofen, Pharmaceut. Dev. Technol. 24 (2019) 947–953, https://doi.org/10.1080/10837450.2019.1572761.
[54] Ž. Vanić, Z. Rukavina, S. Manner, A. Fallarero, L. Uzelac, M. Kralj, D.A. Klarić, A. Bogdanov, T. Raffai, D.P. Virok, J. Filipović-Grčić, N. Škalko-Basnet, Azithromycin-liposomes as a novel approach for localized therapy of cervicovaginal bacterial infections, Int. J. Nanomed. 14 (2019) 5957–5976, https://doi.org/10.2147/IJN.S211691.
[55] Ema, Guideline on the Pharmaceutical Quality of Inhalation and 16 Nasal Medicinal Products, n.d.
[56] E. Casula, M. Manconi, J.A. Vázquez, T.B. Lopez-Mendez, J.L. Pedraz, E. Calvo, A. Lozano, M. Zaru, A. Ascenso, M.L. Manca, Design of a nasal spray based on cardiospermum halicacabum extract loaded in phospholipid vesicles enriched with gelatin or chondroitin sulfate, Molecules 26 (2021), https://doi.org/10.3390/molecules26216670.
[57] M.S. Dykewicz, D.L. Hamilos, Rhinitis and sinusitis, J. Allergy Clin. Immunol. 125 (2010), https://doi.org/10.1016/j.jaci.2009.12.989.
[58] K.A. Foster, C.G. Oster, M.M. Mayer, M.L. Avery, K.L. Audus, Characterization of the A549 Cell Line as a Type II Pulmonary Epithelial Cell Model for Drug Metabolism, 1998.
[59] D. Schutz, C. Conzelmann, G. Fois, R. Groß, T. Weil, L. Wettstein, S. Stenger, A. Zelikin, T.K. Hoffmann, M. Frick, J.A. Muller, J. Munch, Carrageenan-containing over-the-counter nasal and oral sprays inhibit SARS-CoV-2 infection of airway epithelial cultures, Am. J. Physiol. Lung Cell. Mol. Physiol. 320 (2021) L750–L756, https://doi.org/10.1152/ajplung.00552.2020.
[60] M. Böhm, G. Avgitidou, E. El Hassan, R. Mösges, Liposomes: a new non-pharmacological therapy concept for seasonal-allergic-rhinoconjunctivitis, Eur. Arch. Otorhinolaryngol. 269 (2012) 495–502, https://doi.org/10.1007/s00405-011-1696-6.
[61] M. Lauriello, G.P. Di Marco, S. Necozione, C. Tucci, P. Marina, G. Rizzo, A. Eibenstein, Effects of liposomal nasal spray with vitamins a and e on allergic rhinitis, Acta Otorhinolaryngol. Ital. 40 (2020) 217–223, https://doi.org/10.14639/0392-100X-N0357.
[62] S. Song, H. Peng, Q. Wang, Z. Liu, X. Dong, C. Wen, C. Ai, Y. Zhang, Z. Wang, B. Zhu, Inhibitory activities of marine sulfated polysaccharides against SARS-CoV-2, Food Funct. 11 (2020) 7415–7420, https://doi.org/10.1039/d0fo02017f.
[63] M. Gibis, C. Ruedt, J. Weiss, In vitro release of grape-seed polyphenols encapsulated from uncoated and chitosan-coated liposomes, Food Res. Int. 88 (2016) 105–113, https://doi.org/10.1016/j.foodres.2016.02.010.
[64] J. Delgado Adámez, E. Gamero Samino, E. Valdés Sánchez, D. González-Gómez, In vitro estimation of the antibacterial activity and antioxidant capacity of aqueous extracts from grape-seeds (Vitis vinifera L.), Food Control 24 (2012) 136–141, https://doi.org/10.1016/j.foodcont.2011.09.016.
[65] A. Francioso, R. Cossi, S. Fanelli, P. Mastromarino, L. Mosca, Studies on trans-resveratrol/carboxymethylated (1,3/1,6)-β-D-Glucan association for aerosol pharmaceutical applications, Int. J. Mol. Sci. 18 (2017), https://doi.org/10.3390/ijms18050967.
[66] C. Esposito, E.U. Garzarella, B. Bocchino, M. D'Avino, G. Caruso, A.R. Buonomo, R. Sacchi, F. Galeotti, G.C. Tenore, V. Zaccaria, M. Daglia, A standardized polyphenol mixture extracted from poplar-type propolis for remission of symptoms of uncomplicated upper respiratory tract infection (URTI): a monocentric, randomized, double-blind, placebo-controlled clinical trial, Phytomedicine 80 (2021), https://doi.org/10.1016/j.phymed.2020.153368.
[67] A. Abdollahi, N. Fereydouni, H. Moradi, A. Karimivaselabadi, E. Zarenezhad, M. Osanloo, Nanoformulated herbal compounds: enhanced antibacterial efficacy of camphor and thymol-loaded nanogels, BMC Complement Med. Ther. 24 (2024), https://doi.org/10.1186/s12906-024-04435-z.
[68] S. Alghareeb, K. Asare-Addo, B.R. Conway, A.O. Adebisi, PLGA nanoparticles for nasal drug delivery, J. Drug Deliv. Sci. Technol. 95 (2024), https://doi.org/10.1016/j.jddst.2024.105564.
[69] F. Sonvico, A. Clementino, F. Buttini, G. Colombo, S. Pescina, S.S. Guterres, A. R. Pohlmann, S. Nicoli, Surface-modified nanocarriers for nose-to-brain delivery: from bioadhesion to targeting, Pharmaceutics 10 (2018), https://doi.org/10.3390/pharmaceutics10010034.
[70] M.L. Manca, E. Casula, F. Marongiu, G. Bacchetta, G. Sarais, M. Zaru, E. Escribano-Ferrer, J.E. Peris, I. Usach, S. Fais, A. Scano, G. Orrù, R.G. Maroun, A.M. Fadda, M. Manconi, From waste to health: sustainable exploitation of grape pomace seed extract to manufacture antioxidant, regenerative and prebiotic nanovesicles within circular economy, Sci. Rep. 10 (2020), https://doi.org/10.1038/s41598-020-71191-8.
[71] S. Trows, K. Wuchner, R. Spycher, H. Steckel, Analytical challenges and regulatory requirements for nasal drug products in Europe and the U.S, Pharmaceutics 6 (2014) 195–219, https://doi.org/10.3390/pharmaceutics6020195.
[72] Y.S. Cheng, T.D. Holmes, J. Gao, R.A. Guilmette, S. Li, Y. Surakitbanharn, C. Rowlings, Characterization of nasal spray pumps and deposition pattern in a replica of the human nasal airway. Mary Ann Liebert, Inc., 2001.

[73] H. Natsheh, E. Touitou, Phospholipid vesicles for dermal/transdermal and nasal administration of active molecules: the effect of surfactants and alcohols on the fluidity of their lipid bilayers and penetration enhancement properties, Molecules 25 (2020), https://doi.org/10.3390/molecules25132959.
[74] A.O. Elzoghby, Gelatin-based nanoparticles as drug and gene delivery systems: reviewing three decades of research, J. Contr. Release 172 (2013) 1075–1091, https://doi.org/10.1016/j.jconrel.2013.09.019.
[75] L. Illum, Nasal drug delivery - possibilities, problems and solutions, J. Contr. Release (2003) 187–198, https://doi.org/10.1016/S0168-3659(02)00363-2.
[76] A. Seifelnasr, X.A. Si, J. Xi, Visualization and estimation of nasal spray delivery to olfactory mucosa in an image-based transparent nasal model, Pharmaceutics 15 (2023), https://doi.org/10.3390/pharmaceutics15061657.
[77] H. Harbeoui, A. Hichami, W.A. Wannes, J. Lemput, M.S. Tounsi, N.A. Khan, Anti-inflammatory effect of grape (Vitis vinifera L.) seed extract through the downregulation of NF-κB and MAPK pathways in LPS-induced RAW264.7 macrophages, South Afr. J. Bot. 125 (2019) 1–8, https://doi.org/10.1016/j.sajb.2019.06.026.
[78] L. Illum, Nasal drug delivery—possibilities, problems and solutions, J. Contr. Release 87 (2003) 187–198, https://doi.org/10.1016/S0168-3659(02)00363-2.
[79] A. Rygg, M. Hindle, P.W. Longest, Absorption and clearance of pharmaceutical aerosols in the human nose: effects of nasal spray suspension particle size and properties, Pharm. Res. 33 (2016) 909–921, https://doi.org/10.1007/s11095-015-1837-5.
[80] M. Gao, X. Shen, S. Mao, Factors influencing drug deposition in the nasal cavity upon delivery via nasal sprays, J. Pharm. Investig. 50 (2020) 251–259, https://doi.org/10.1007/s40005-020-00482-z.
[81] E. Touitou, S. Duchi, H. Natsheh, A new nanovesicular system for nasal drug administration, Int. J. Pharm. 580 (2020) 119243, https://doi.org/10.1016/j.ijpharm.2020.119243.
[82] S.K. Pitta, N. Dudhipala, A. Narala, K. Veerabrahma, Development of zolmitriptan transfersomes by Box–Behnken design for nasal delivery: *in vitro* and *in vivo* evaluation, Drug Dev. Ind. Pharm. 44 (2018) 484–492, https://doi.org/10.1080/03639045.2017.1402918.
[83] B. Hazt, D.J. Read, O.G. Harlen, W.C.K. Poon, A. O'Connell, A. Sarkar, Mucoadhesion across scales: towards the design of protein-based adhesives, Adv. Colloid Interface Sci. 334 (2024), https://doi.org/10.1016/j.cis.2024.103322.